J. Anat. (2007) **210**, pp54–65 doi: 10.1111/j.1469-7580.2006.00671.x

Reactive changes of retinal astrocytes and Müller glial cells in kainate-induced neuroexcitotoxicity

Min-Lin Chang,[1] Ching-Hsiang Wu,[2] Ya-Fen Jiang-Shieh,[3] Jeng-Yung Shieh[1] and Chen-Yuan Wen[1]

[1]*Department of Anatomy and Cell Biology, College of Medicine, National Taiwan University, Taipei, Taiwan*
[2]*Department of Biology and Anatomy, National Defense Medical Center, Taipei, Taiwan*
[3]*Department of Anatomy, College of Medicine, National Cheng Kung University, Taiwan*

Abstract

The aim of this study was to investigate reactive changes of astrocytes and Müller glial cells in rats subjected to kainate treatment, which leads to neuronal degeneration in the ganglion cell layer and the inner border of the inner nuclear layer as confirmed by labelling with Fluoro-Jade B, a marker for degenerating neurons and fibres. Both the astrocytes and the Müller glial cells reacted vigorously to kainate injection as shown by their up-regulated expression of nestin, glial fibrillary acidic protein and glutamine synthetase. A major finding was the induced expression of nestin together with glial fibrillary acidic protein beginning at 1 day post-injection of kainate. The marked nestin expression appeared to be most intense at 1 day and was sustained till 2 weeks as compared with the untreated/normal retina. Western blotting analysis confirmed a marked increase in expression of nestin, glial fibrillary acidic protein and glutamine synthetase as compared with untreated/normal retina. Double labelling study revealed that astrocytes and Müller glial cells expressed the radial glia marker nestin, and incorporated bromodeoxyuridine to re-enter into their cell cycle. The induced expression of these proteins in astrocytes and Müller glial cells indicated an induction of gliotic responses and de-differentiation that may be associated with regenerative efforts after kainate-induced injury. Indeed, with the acquisition of an immature molecular profile as manifested by the induced expression of brain lipid-binding protein and doublecortin in astrocytes and Müller glial cells, the potential of these cells to de-differentiate in retinal neurodegeneration is greatly amplified.

Key words astrocytes; de-differentiate; GFAP; GS; kainate; Müller glial cells; nestin.

Introduction

There are two types of macroglial cells in the mammalian retina, namely astrocytes and Müller glial cells (Newman, 2001). Astrocytes appear to originate in the optic nerve head and subsequently migrate to the nerve fibre layer (NFL) and ganglion cell layer (GCL) (Norton et al. 1992). They are restricted to the vitreal surface of the retina, where they are located largely within the NFL and thought to play a pivotal role in neuronal signalling and in maintaining endothelial barrier properties (Ridet et al. 1997). By contrast, the Müller glial cells, specialized radial glial cells that extend from the inner limiting membrane to the outer liming membrane, provide functional and structural support to the retinal neurons and regulate the neuronal function through various mechanisms including potassium siphoning and glutamate metabolism (Newman & Reichenbach, 1996).

The best known markers, among others reflecting altered glial reactivity in the retina, are glial fibrillary acidic protein (GFAP) and glutamine synthetase (GS) (Lam et al. 1995; Chen & Weber, 2002). GFAP is a 51-kDa intermediate filament protein found in the astrocytes, Müller glial cell end-feet and processes. Although Müller glial cells in normal rat retinas express little or no GFAP (Bignami & Dahl, 1979), they showed increased GFAP expression in retinal injuries including ischaemia (Larsen & Osborne, 1996), glaucoma (Xue et al. 2006) and kainate-induced neuronal death (Honjo et al. 2000). GS

Correspondence
Professor Chen-Yuan Wen, Department of Anatomy and Cell Biology, National Taiwan University, 1, Sec. 1, Jen Ai Road, Taipei 100, Taiwan. T: +886 2 3562211; F: +886 2 3915292; E: wcywn@ha.mc.ntu.edu.tw

Accepted for publication *25 September 2006*

is found in Müller glial cell soma and plays an important role in controlling the level of extracellular glutamate. Although GS was considered to be exclusively expressed in Müller glial cells (Riepe & Norenburg 1977), Derouiche & Rauen (1995) also found positive GS immunoreactivity in rat retinal astrocytes. Recently, several studies have shown that the expression of nestin is induced in reactive astrocytes (Frisen et al. 1995) of the brain and Müller glial cells of the retina (Xue et al. 2006). Nestin is a characterized class IV intermediate filament expressed in the early central nervous system (CNS) (Lendahl et al. 1990) first described in the neural tube (Hockfield & Mckay, 1985). It has long been used as a cell distinguishing marker for radial glia and now is increasingly used as a marker for neural progenitor cells. It has been reported that injection of a potent exitocin, kainate, into the rat vitreous humor can cause the retina to undergo severe neural degeneration (Honjo et al. 2000). It remains to be determined whether the expression levels of GFAP, GS and nestin in astrocytes and Müller glial cells that are known to be altered in different retinal damage would be similarly affected and, if so, to investigate their progressive changes in kainate-induced neurotoxicity. In addition, molecules related to neural progenitors such as brain lipid-binding protein (BLBP) and doublecortin (DCX) were also examined. The information obtained may help better to understand the roles of astrocytes and Müller glial cells in retinal degeneration and regeneration.

Materials and methods

Animals and tissue processing

Adult male Wistar rats weighing 250–350 g (~8–10 weeks old; $n = 85$) were used in this study. All experiments were conducted in accordance with the standards of the Association for Research in Vision and Ophthalmology. The intravitreal injection procedure has been described in detail previously (Honjo et al. 2000). Briefly, rats were anaesthetized with an intraperitoneal injection of 7% chloral hydrate (0.3 g kg^{-1}). Kainic acid (KA; Sigma, St Louis, MO, USA, K0250) was dissolved in sterile normal saline solution administered at a concentration of 5 nM. Each rat was given an intravitreal injection of 1.4 μL KA into the right eye. The same volume of sterile 0.9% normal saline was injected into the left eye as the controls. The experimental animals were killed at 1, 3, 7 and 14 days after injections. Eight rats were used for each time point (including the untreated/normal group). All rats were anaesthetized with 7% chloral hydrate injected intraperitoneally. The rats were first perfused with Ringer's solution until the lungs and livers were cleared of blood, and then followed by 4% paraformaldehyde in 0.1 M phosphate buffer (PB; pH 7.4). After fixation, the eyes were freshly removed and immediately the lens, vitreal body and connective tissue were detached before transfer into 30% sucrose solution and were kept in the same solution overnight at 4 °C. Sagittal cryostat sections of 12 μm thickness were prepared and mounted on micro slides (Dako, Carpinteria, CA, USA; 5116) and air-dried. Mounted sections were observed microscopically and images at a distance about 1 mm around the optic disc were selected for morphological and immunohistochemical study.

Fluoro-Jade B (FJB) staining

FJB staining is a well-established method to mark degenerating neurons and fibres (Schmued et al. 1997). Mounted sections were first immersed in a solution containing 1% sodium hydroxide in 80% alcohol for 5 min, followed by 70% alcohol and distilled water each for 2 min. The sections were then transferred to a solution of 0.06% potassium permanganate for 20 min, and rinsed several times in distilled water. The staining solution was prepared from a 0.01% stock solution of FJB (Chemicon, Temecula, CA, USA, AG310) that was made by adding 10 mg of the dye powder to 100 mL of distilled water. To make up 100 mL of working solution, 4 mL of the stock solution was added to 96 mL of 0.1% acetic acid vehicle, resulting in a final dye concentration of 0.0004%. After 20 min incubation in the working solution, the sections were washed several times in distilled water each for 5 min, and examined in a fluorescence light microscope using green light (500–570 nm) excitation.

Immunohistochemistry

Mounted sections were first treated in a solution containing 10% methanol and 1% hydrogen peroxide in Tris-buffered saline (TBS) for 1 h. After this, the sections were blocked in a combination of 0.1% Triton X-100 and 10% normal horse serum (NHS) or normal goat serum (NGS) for 1 h. They were then incubated overnight with the following primary antibodies: GS (1 : 500, Chemicon, MAB302), GFAP (1 : 1000, Chemicon, AB5804) and nestin (1 : 100, Chemicon, MAB353). After incubation, sections

were treated with the secondary antibody, biotinylated horse anti-mouse IgG (1 : 200; Vector, Burlingame, CA, USA, BA2001) or goat anti-rabbit IgG (1 : 200, Vector, BA1000), for 1 h. The reaction was amplified with streptavidin–biotin–peroxidase complex (1 : 300; Dako, P0387) and visualized with 3,3-diaminobenzidine tetrahydrochloride (DAB; Sigma, D-5637). All sections were counterstained by cresyl fast violet and examined under the light microscope (Zeiss, Axiophot). For double labelling, mounted sections were blocked in TBS containing 10% NGS for 1 h, and then incubated with a mixture of two of the following primary antibodies: GS, GFAP, nestin, BLBP (1 : 50, Chemicon, AB9558), DCX (1 : 50, Santa Cruz Biotechnology, Inc., Santa Cruz, CA, USA, SC8066) and bromodeoxyuridine (BrdU; 1 : 100, Chemicon, MAB3510) overnight, and then followed by a dilution (1 : 100) of fluorescein isothiocyanate (FITC)-conjugated goat anti-mouse/donkey anti-goat IgG (Jackson ImmunoResearch, 115-095-003/705-095-003) or rhodamine (TRITC)-conjugated goat anti-mouse/goat anti-rabbit IgG (Jackson ImmunoResearch, Stratech Scientific Ltd, Newmarket, UK, 115-025-003/111-025-003), for 2 h. The sections were then counterstained by 4′,6-diamidino-2-phenylindole (DAPI; Molecular Probes, D-1306), and then examined under a confocal laser-scanning microscope (Leica, TCS SP2, Germany). The sections were illuminated by light with an excitation wavelength of 488 nm for FITC, 568 nm for TRITC and UV light for DAPI.

Western blot

Forty-five rats, three (including the untreated/normal group) for each time point were used. Rats were killed by an overdose of 7% chloral hydrate. The eyeballs were immediately removed and the retinas were isolated before being transferred into dry ice and stored at –80 °C until use. Briefly, isolated retinas were homogenized in a lysine buffer containing 10% protease inhibitor cocktail (Sigma, P8340) and then sonicated. The homogenate was centrifuged; supernatant was collected and the pellet was re-suspended in homogenization buffer. A fourth volume of 4× reducing SDS sample buffer was added to the lysates and boiled at 95 °C for 5 min. Protein samples (50 μg protein per gel lane) (protein determined by Bio-Rad protein Kit, Bio-Rad Laboratory, Hercules, CA, USA) were separated on 10% (for GS and GFAP) or 7.5% (for nestin) acrylamide-SDS gels, and electrotransferred to nitrocellulose membrane (Bio-Rad). Non-specific sites were blocked by incubating the membrane with TBS containing 5% NGS and 0.1% Tween 20 for 2 h and incubated with primary antibodies at 4 °C overnight: GS, GFAP and nestin. After washing with TBST (TBS containing 0.1% Tween 20), membranes were incubated with horseradish peroxidase-conjugated secondary anti-mouse (1 : 5000, Santa Cruz, sc- 2001) or antirabbit (1 : 5000, Santa Cruz, sc-2004) for 2 h. Specific binding was revealed by Western blotting luminal reagent (Santa Cruz, sc-2048). For loading control, the membranes were reprobed with a monoclonal anti-β-actin (1 : 1000, Sigma, A5441) or anti-β-tubulin (1 : 1000, Santa Cruz, sc-5286) and revealed as mentioned above. Molecular weights were estimated by using a prestained protein ladder (Bioman, PREP1025). The density of reactive bands was scanned (Scan marker 8700, MICROTEK) and quantified by densitometry using Gel pro 3.1 (Media cybernetics, Silver Spring, MD, USA).

Western blot quantification

The Western blots used for statistical analysis were repeated at least three times for each group (GS, GFAP and nestin). The density of the untreated/normal group (untreated/normal retina) was defined as 100% and the densities of the other groups were expressed as a percentage of this value. The optical density was also obtained. All data were then evaluated with ANOVA and Student's *t*-test for statistical significance. Differences were considered significant at $P < 0.05$. Comparisons were made between untreated/normal and control/each KA groups.

Results

Cell death revealed by FJB staining in KA-intoxicated retinas

When compared with that of saline-treated rats (Fig. 1A), the retina in rats receiving KA injection and killed at 1 day appeared structurally normal (Fig. 1B) and showed many FJB-labelled cells localized mainly in the GCL and the inner border of the inner nuclear layer (INL). At 3 days after KA injection, the NFL, GCL and IPL began to shrink and contained many FJB-stained cells (Fig. 1C). The attenuated NFL, GCL and IPL were hardly discernible at 7 and 14 days post-injection and collectively are referred to as ANGI, in the inner zone of which many of the FJB-labelled cells were found (Fig. 1D,E).

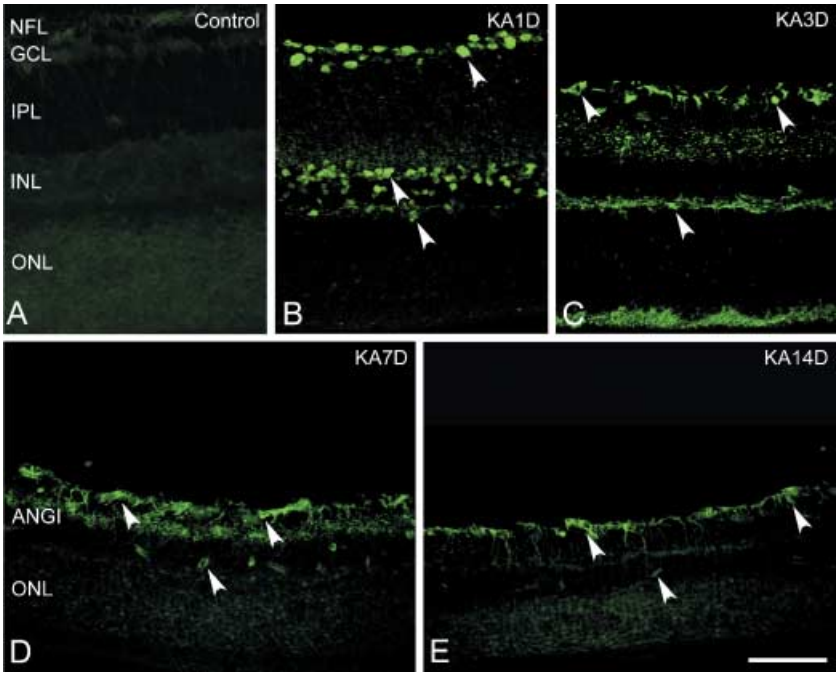

Fig. 1 FJB staining in the retinas following saline (A) or KA (B–E) injection. FJB-labeled neurons are absent in the control retina (A). Many FJB-labelled neurons are localized in the GCL and INL at 1 and 3 days after KA injection (B,C, arrowheads). At the latter time interval, many FJB-stained cells are also detected in the ANGI (D,E, arrowheads). NFL, nerve fibre layer; GCL, ganglion cell layer; IPL, inner plexiform layer; INL, inner nuclear layer; ONL, outer nuclear layer; ANGL, attenuated NFL, GCL, IPL and INL. Scale bar = 50 μm.

Glial responses in the rat retinas challenged with KA: assessment with GS, GFAP and nestin immunoreactivities

In untreated/normal as well as saline-treated retinas (Fig. 2A,B), intense GS immunoreactivity was localized in the Müller glial cell end-feet and astrocytes in the GCL and NFL. At 1 day after KA injection, very strong GS immunoreactivity was found not only in the basal Müller glial cell processes and astrocytes within the GCL and NFL, but also in Müller glial cell bodies especially in the INL (Fig. 2C). GS immunoreactivity remained elevated in the inner retina at day 3 post-injection (Fig. 2D). By 1–2 weeks post-injection, the pattern of GS staining was reduced and similar to that in the normal or controls (Fig. 2E,F). Western blot analysis was consistent with the immunohistochemical results, which show that the levels of total GS protein were drastically increased at 3 days post-injection, but declined thereafter (Fig. 2G).

Astrocytes and Müller glial cells from untreated/normal (Fig. 3A) as well as saline-treated rats (Fig. 3B) showed a low level of GFAP immunoreactivity. The pattern and level of GFAP staining were mildly affected at 1 day after KA injection (Fig. 3C). Subsequently, GFAP immunoreactivity was gradually increased, and heavily labelled processes could be seen extending across the inner part of the ANGI (Fig. 3D). GFAP staining was markedly increased at day 7 and 14, when heavily labelled processes could be seen in parallel arrays now extending across the entire width of the retina (Fig. 3E,F). The somata of the Müller glial cells within the INL did not show a well-defined GFAP staining at any of the time points studied. Consistent with the immunohistochemical results, Western blot analysis also showed a gradually increased level of total GFAP protein after KA injection during the experimental period examined (Fig. 3G).

Nestin-positive cells were elongated with slender processes and were restricted primarily within the NFL and GCL in the untreated/normal retina (Fig. 4A). Enhanced nestin immunoreactivity was observed in some radial processes extending into the IPL after saline injection (Fig. 4B). At 1 day post-injection, nestin-positive radial processes extended further to the outer limiting membrane (Fig. 4C). Nestin immunoreactivity was markedly increased and the immunopositive processes were tortuous and stout. After this time, immunoreactivity was gradually decreased up to 2 weeks after KA injection (Fig. 4D–F). Western blot analysis showed that the levels of total nestin protein were drastically increased at day 1 as compared with those in the untreated/normal retina, and then decreased gradually thereafter (Fig. 4G).

In view of the significant increase of nestin, GS and GFAP in astrocytes and Müller glial cells at 3 days post-

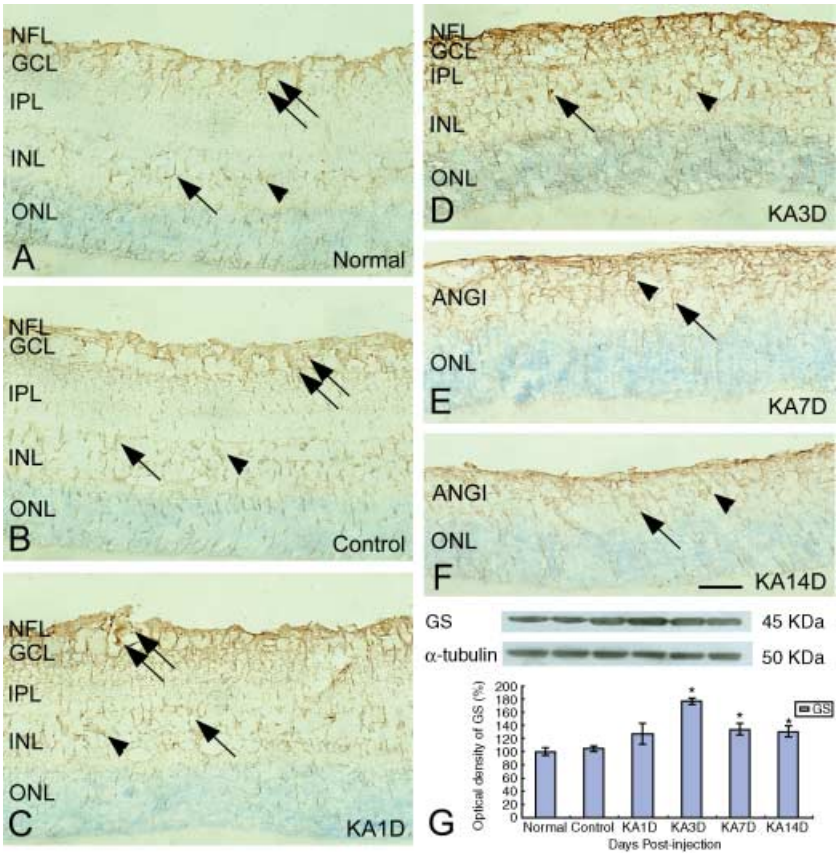

Fig. 2 GS immunoreactivity in the untreated/normal retina (A), and those following saline (B) and KA (C–F) injections. In the untreated/normal or saline-treated retinas, GS immunoreactivity is most intense at astrocytes and the end-feet of Müller glial cells adjacent to the ganglion cells (A,B, double arrows). In rats given KA injection and killed at 1 and 3 days, the intense GS immunoreactivity appears not only in the NFL and GCL (C,D, double arrows), but also in the INL. At all time points, GS-labelled processes appear to span the whole retina (A–F, arrows), whereas GS-positive cell somata of Müller glial cells reside within the INL (A–F, arrowheads). (G) Expression of total GS protein quantified by immunoblot in the untreated/normal, saline- and kainate-treated retinas. The levels of total GS protein are drastically increased at 1 day after KA injection peaking at 3 days but declining thereafter. *Significant difference ($P < 0.05$) as compared with the untreated/normal groups ($n = 3$). Other abbreviations as in Fig. 1; scale bar = 50 μm (applies to A–F).

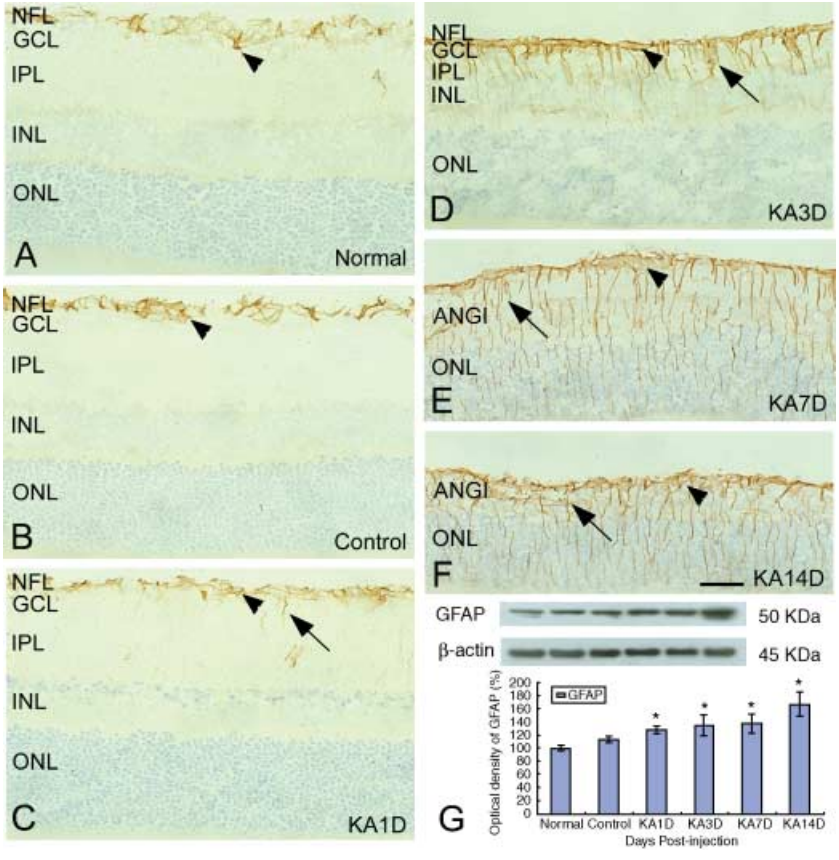

Fig. 3 GFAP immunoreactivity in the retinas of the untreated/normal rats (A), and those after saline (B) and KA (C–F) injections. In the untreated/normal and saline-treated retinas, GFAP immunoreactivity is restricted primarily to the NFL and GCL (A,B, arrowheads). GFAP expression is moderately increased at 1 day post-injection (C, arrowheads) and noticeably enhanced at 3 days after KA injection (D, arrowheads). At 1 and 3 days, GFAP-labelled processes extend across the inner part of the inner retina (C,D, arrows). Increased GFAP expression is sustained at 7 days, and is most pronounced at 14 days (E,F, arrowheads). Meanwhile, heavily labelled processes extend across the entire width of the retina (E,F, arrows). (G) Expression of total GFAP protein quantified by immunoblot in the untreated/normal, saline- and KA-treated rats. The levels of total GFAP protein increase gradually, beginning at 1 day until 2 weeks posinjection. *Significant difference ($P < 0.05$) when compared with the untreated/normal groups ($n = 3$). Abbreviations as in Figs 1 and 2; scale bar, 50 μm (A–F).

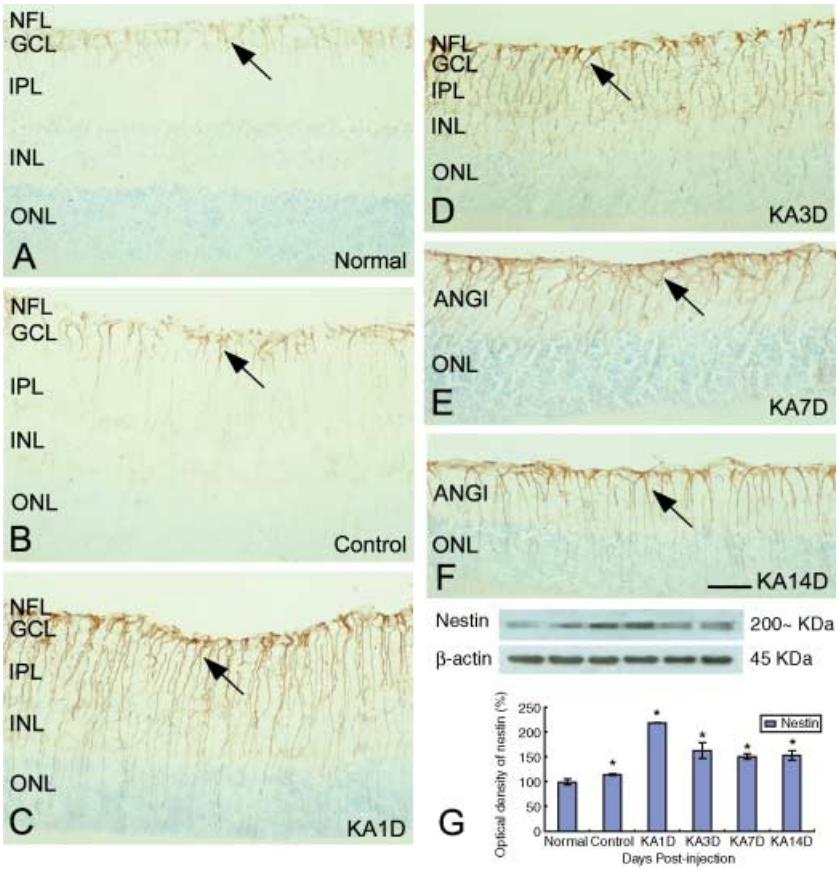

Fig. 4 Nestin immunoreactivity in the retinas of untreated/normal rats (A), and those after saline (B) and KA (C–F) injections. In the untreated/normal retina, nestin labelling is mainly localized to the NFL and GCL (A, arrow). After saline injection, nestin-positive processes extend into the IPL (B, arrow). At 1 day post-injection, nestin immunoreactivity is dramatically increased, and labelled radial processes that are tortuous and stout extend across the whole retina (C, arrow). Nestin immunoreactivity is then reduced up to 2 weeks after KA injection (D–F, arrows). (G) Expression of total nestin protein quantified by immunoblot in the untreated/normal, saline- and KA-treated rats. When compared with that in the untreated/normal rats, the levels of total nestin protein are drastically increased at 1 day post-injection; however, they decline gradually thereafter. *Significant difference ($P < 0.05$) when compared with the untreated/normal groups ($n = 3$). Abbreviations as in Figs 1 and 2; scale bar, 50 μm (A–F).

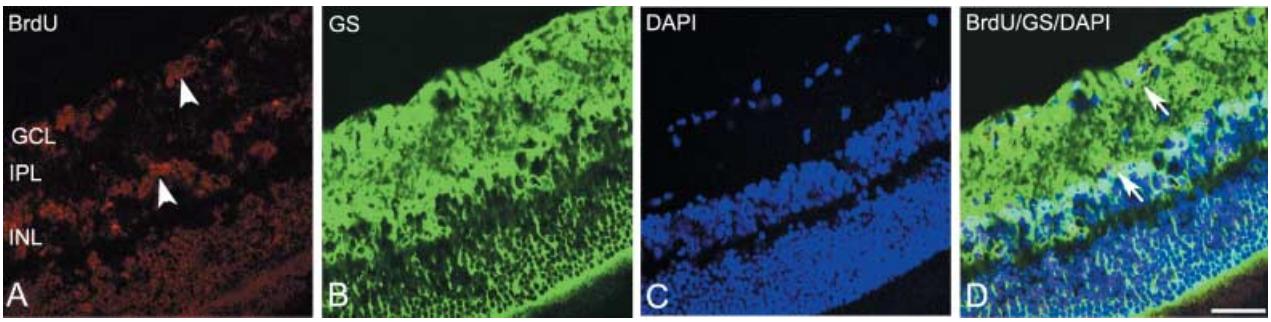

Fig. 5 Confocal images of BrdU and GS immunolabelling in KA-injected retina at 3 days (A–D) post-injection. BrdU-immunolabelled cells (A; red, arrowheads) are located in the GCL and INL at 3 days post-injection. Astrocytes and Müller glial cells are marked with biotinylated anti-GS antibody detected with goat anti-rabbit IgG-conjugated FITC (B; green), and the cell nuclei are counterstained by DAPI (C; blue). The merged images show that astrocytes and Müller glial cells containing GS concurrently express BrdU immunoreactivity (D; yellow, arrows) in the injured retina. Abbreviations as in Figs 1 and 2; scale bar, 40 μm.

injection, it was important to ascertain if the increased amount of proteins was in part due to the proliferation of astrocytes and Müller glial cells. Double labelling of BrdU with GS at this time point was carried out. We found that BrdU-labelled cells were mainly located in the GCL and INL (Fig. 5A) and these cells also concurrently expressed GS (Fig. 5B–D) at 3 days post-injection.

Co-localization of nestin, BLBP and DCX immunoexpression in astrocytes and Müller glial cells in KA-injected retinas

To ascertain if nestin, BLBP and DCX were all expressed in astrocytes and Müller glial cells other than in neurons, double labelling between the proteins was carried out.

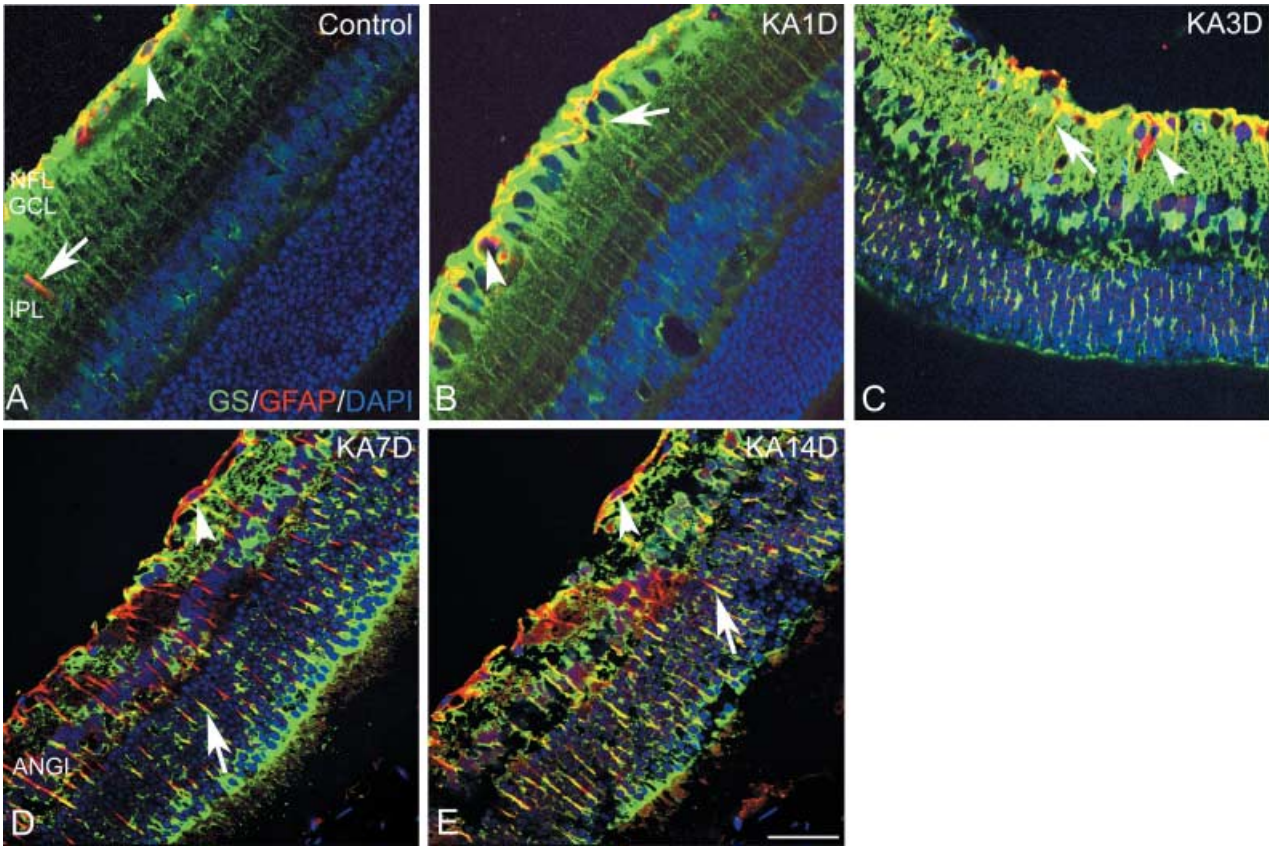

Fig. 6 Confocal images of GFAP (red) and GS (green) immunolabelling in saline- (A) or KA-treated retinas (B–E). GFAP labelling is localized in Müller glial cell end-feet (A, arrow) and the cell body of some astrocytes (A, arrowhead) in the control retina. Astrocytes and Müller glial cells in lesioned retinas concurrently express GFAP and GS immunoreactivities that are localized mainly in the cell processes (B–E, arrows); some cell bodies located in the inner retina also concomitantly express GFAP and GS immunoreactivities (B–E, arrowheads). Abbreviations as in Figs 1 and 2; scale bar, 40 μm.

In the control retina and retinas at 1 day post-injection, GFAP immunoreactivity restricted in the NFL and GCL was concurrently stained by GS ($GFAP^+/GS^+$, Fig. 6A,B). At the later time intervals, co-localization of GFAP with GS immunoreactivity was frequently found (Fig. 6C–E). $GFAP^+/GS^+$ processes were gradually increased in intensity and appeared to extend across the entire width of the ANGI. In the control retina, nestin immunoreactivities were restricted within the NFL and GCL; a few of these areas were co-labelled with GFAP ($GFAP^+/nestin^+$, Fig. 7A) or GS ($GS^+/nestin^+$, Fig. 8A). Interestingly, the distribution pattern of nestin was increased gradually and overlapped that of GFAP (Fig. 7B) or GS (Fig. 8B) from day 1 post-injection. Nestin coupled with GFAP- (Fig. 7C–E) or GS- (Fig. 8C–E) stained processes were also observed at later time intervals of KA challenge. BLBP (Fig. 9A) or DCX (Fig. 10A) immunoreactivity was not detected in the retinas of control rats. However, induced BLBP and DCX immunoreactivities were detected and overlapped those of GFAP, $GFAP^+/BLBP^+$ (Fig. 9B) and $GFAP^+/DCX^+$ (Fig. 10B), respectively, at day 1 post-injection. Increased overlapping of GFAP immunoreactivity with that of BLBP (Fig. 9C) or DCX (Fig. 10C) was still observed from day 3 post-injection and remained so at the later time intervals (Figs 9D,E and 10D,E).

Discussion

Radial glial cells appear early and display a bipolar shape with processes spanning along the full width of the developing CNS. The cell bodies are mainly situated in the ventricular or subventricular zones in which a short process anchors the cell soma to the lumen, while an elongated process reaches the pial surface (Rakic, 1995). The cells function as a scaffold upon which newborn neurons migrate, and as neuronal progenitors (Anthony et al. 2004; McDermott et al. 2005), as reflected by the existence of the neural precursor cell marker nestin (Frederiksen & McKay, 1988). Radial glial cells also contain specific proteins found in mature

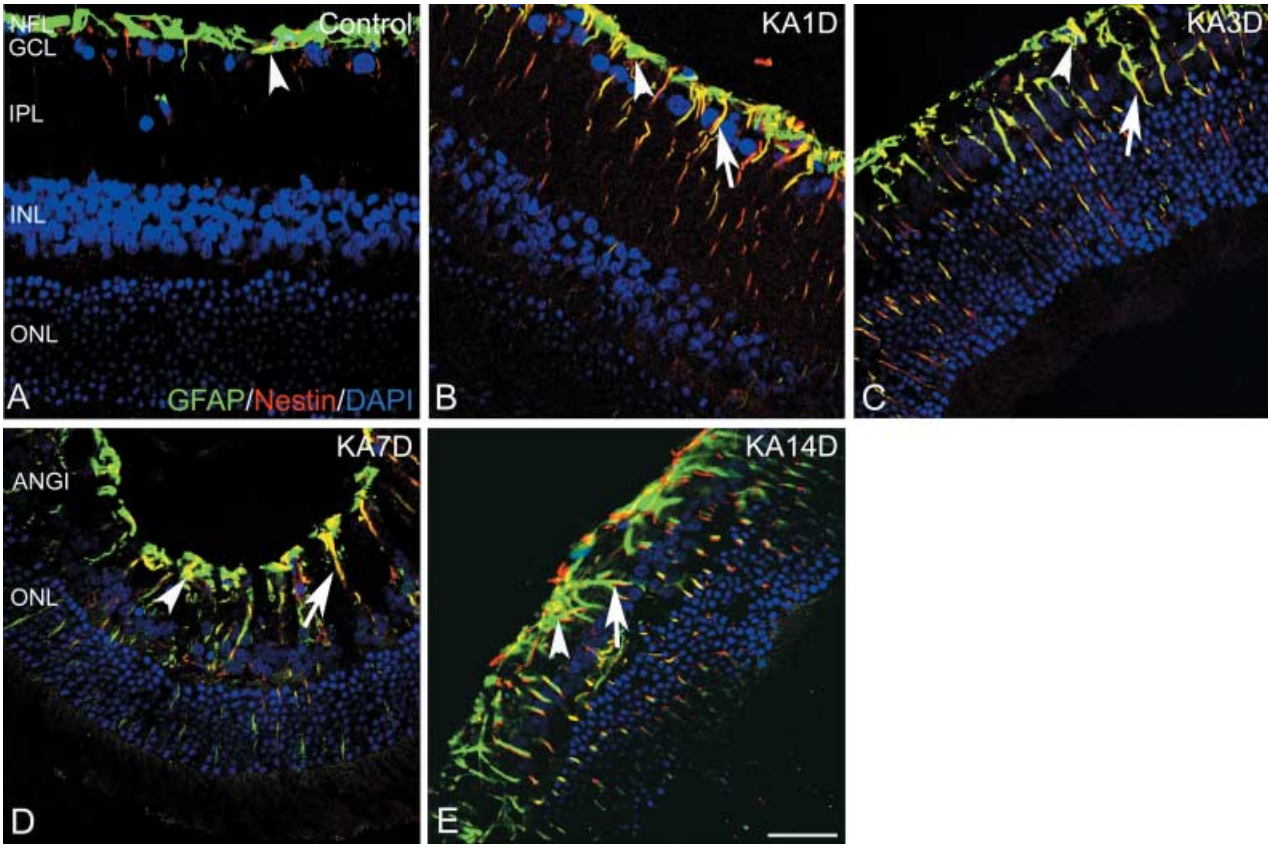

Fig. 7 Confocal images of GFAP (green) and nestin (red) immunolabelling in rats receiving saline (A) or KA (B–E) injections. Astrocytes and Müller glial cells especially in the lesioned retinas (B–E) express both GFAP and nestin immunoreactivities that are localized primarily in their processes (arrows). Immunoreactivities are also detected in some cell bodies in the inner retina (arrowheads). Abbreviations as in Figs 1 and 2; scale bar = 40 μm.

astrocytes such as GS, vimentin, BLBP and glutamate aspartate transporter (GLAST) (Hartfuss et al. 2001; Götz & Barde, 2005). GLAST- and BLBP-positive radial glial cells have been shown to express nestin until their morphological transformation into astrocytes when nestin is down-regulated (Hartfuss et al. 2001). The morphological transformation of radial glia into astrocytes appears to coincide with the loss of vimentin protein and acquisition of GFAP (Voigt, 1989). In the mature CNS, the cerebellum and retina retain characteristic radial glial cells as the Bergmann glia and Müller glia, respectively, which may regulate synaptic plasticity and participate in a bidirectional communication with neurons (Morest & Silver, 2003).

Nestin and DCX are well known to be markers of neural progenitor cells, but not expressed by differentiated neurons (Hatten, 1990, 1999; Brown et al. 2003). In the mature mammalian retina, nestin-positive cells are very low in number and are mainly located in the pigmented ciliary bodies (Ahmad et al. 2000; Tropepe et al. 2000). Recent study also revealed the existence of nestin-positive cells in the retina, which were regarded as retinal progenitor cells (Walcott & Provis, 2003). In our present study in KA-induced retinal injury, both immunohistochemical and Western blot data indicated a significantly higher level of nestin expression in astrocytes and Müller glial cells within 1 day after KA injection as compared with that in the untreated or normal retinas. Although the number of FJB-labelled dying cells in the injured retinas was markedly increased at the same time, no obvious structural alterations were found till 3 days post-injection. It would appear therefore that induced and enhanced nestin expression in astrocytes and Müller glial cells preceded the onset of neurodegeneration or neuronal loss. In glaucomatous rats, the induced expression of nestin with a rise of intraocular pressure began at 2 h (Xue et al. 2006), suggesting that retinal astrocytes and Müller glial cells are highly sensitive to retinal damage that may precede definite neuronal cell death. In other words, the glia

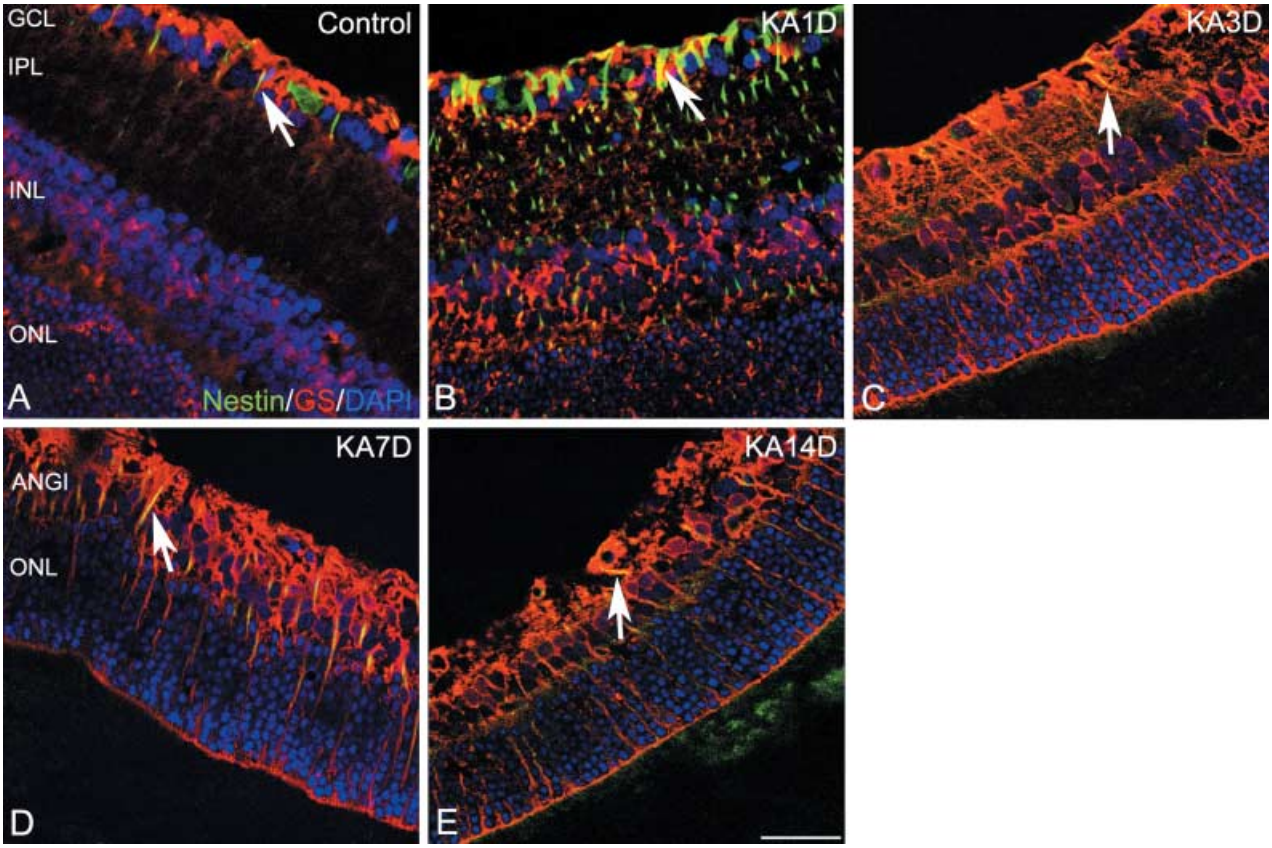

Fig. 8 Confocal images of GS (red) and nestin (green) immunolabelling in rats receiving saline (A) or KA (B–E) injections. GS immunoreactivity is confined to Müller glial cell somata and processes (A, arrow) in the control retina in which nestin immunoreactivity is hardly detected. After KA injection, astrocytes and Müller glial cells enhance both GS and nestin immunoreactivities localized mainly in their processes (B–E, arrowheads). Abbreviations as in Figs 1 and 2; scale bar, 40 μm.

may act as neuropathology sensors for detection of subtle changes in their ambient environment (Xue et al. 2006).

Previous results have shown mRNA expression of two astroglial marker genes GFAP and vimentin in CNS of hens treated with diisopropylphosphrofluoridate (Damodaran & Abou-Donia, 2000). These authors also found continued expression of vimentin in the cerebral astrocytes and further suggested that the cells may de-differentiate to increase vimentin expression for survival. In embryonic neurons transplanted into an adult mouse neocortex model, Leavitt et al. (1999) found a population of adult host glial cells which showed coexpression of RC2 and β-galactosidase in cortical areas adjacent to migrating donor neurons and transiently de-differentiated to a developmentally regulated transitional radial glial phenotype. Kohno et al. (2006) suggested that induction of nestin, Ki-67 and cyclin D1 expression in adult retinal Müller glial cells may be due to their de-differentiation and proliferation in response to laser injury. In our present results, nestin, BrdU and GS expressions peaked at an early stage (3 days) of KA injection. Double labelling of BrdU and GS indicated that astrocytes and Müller glial cells in KA-challenged retinas may undergo proliferation, a hallmark of de-differentiation. Taken together, these studies suggest that an astrocyte cell lineage including retinal astrocytes and Müller glial cells can undergo de-differentiation and proliferation as required to become progenitors and provide regenerative efforts.

As a marker for neural progenitor cells, DCX was transiently expressed in neuronal-determined precursors and was down-regulated during neuronal maturation (Brown et al. 2003). The view that neuronal specificity of DCX is limited to the normal developing nervous system has been questioned. Recent studies have shown a co-expression of DCX with glial markers (S100-protein, GFAP) in gliomas (Daou et al. 2005; Bernreuther et al. 2006) and an acquisition of DCX associated with migratory neuroblasts for oligodendrocyte precursor cells engrafted to the hippocampus *in vivo* (Gaughwin et al.

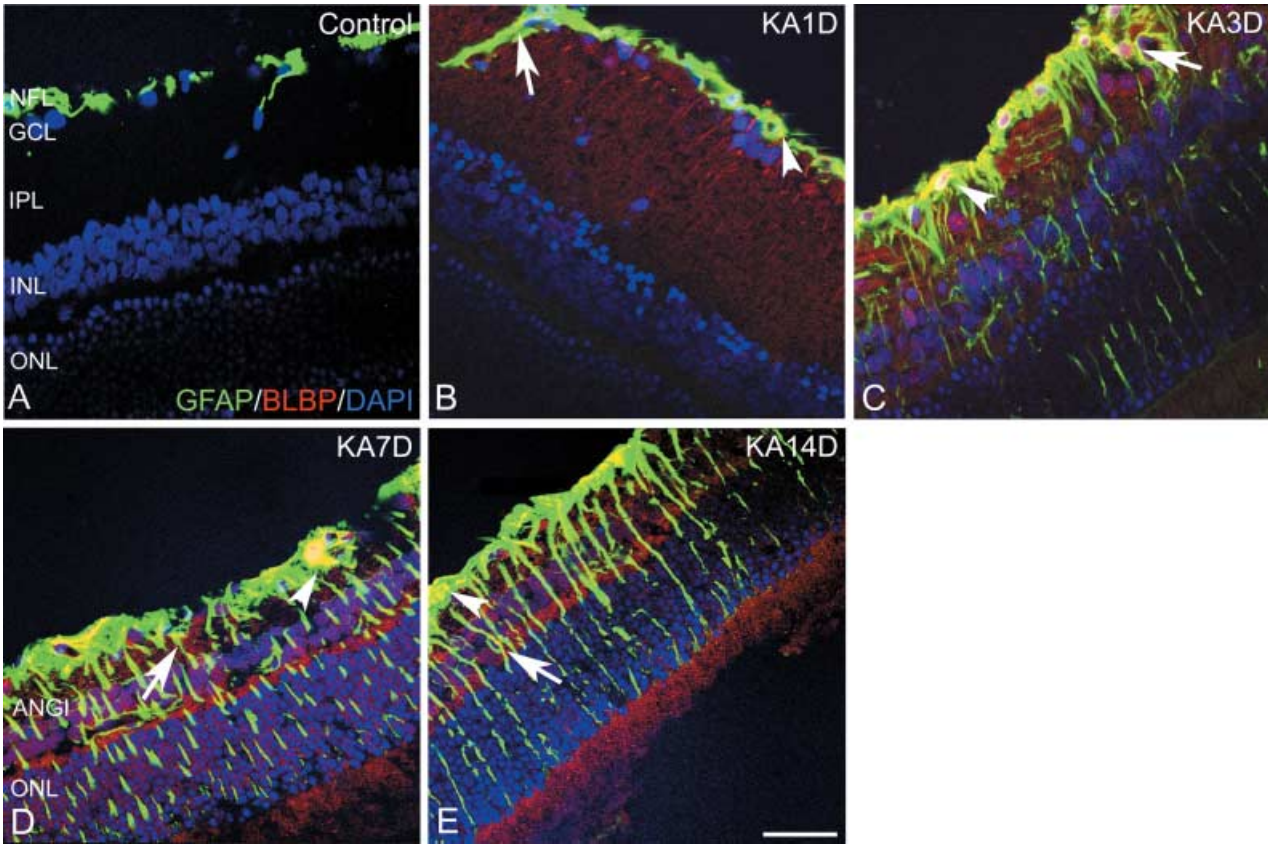

Fig. 9 Confocal images of GFAP (green) and BLBP (red) immunolabelling in retinas after saline (A) or KA (B–E) injection. BLBP staining is not detected in the control retina (A). After KA injection, GFAP-labelled astrocytes and Müller glial cells express BLBP immunoreactivities that are mostly localized in the cell processes (B–E, arrows), and occasionally in the cell bodies within the inner retina especially at 3 and 7 days post-injection (C,D, arrowheads). Abbreviations as in Figs 1 and 2; scale bar = 40 μm.

2006). In the present study, DCX immunoreactivity was induced in retina challenged with KA, and was increased with the development of injury. Interestingly, DCX immunoreactivity was obviously co-localized with that of GFAP during KA treatment, indicating a significant induction of DCX in retinal astrocytes and Müller glial cells after KA-induced neuroexcitotoxicity. A similar induced expression pattern of BLBP and its overlapping with that of GFAP in astrocytes and Müller glial cells was observed in the present study. It has been proposed that BLBP, another radial glia marker, functions in the interaction and signalling between neurons and glia. Moreover, it also facilitates neuronal differentiation, migration or axon extension in the developing brain (Feng et al. 1994; Miller et al. 2003). BLBP is developmentally regulated in the embryonic chick retina and it is barely detected in the adult (Sellner, 1994). However, cellular localization of BLBP was not definitive, especially as it was expressed by Müller glial cells in the embryonic chick retina (Sellner, 1993) and in the retinal spheres of the postnatal rats (Engelhardt et al. 2004). By contrast, it is unequivocal that BLBP was expressed in immature Müller glia of zebrafish embryos and that it was down-regulated with glial maturation in the adult zebrafish (Raymond et al. 2006). When the retina of zebrafish was injured, the nuclei of activated Müller glia moved towards the apical surface and re-expressed BLBP, suggesting de-differentiation (Raymond et al. 2006). Our present results have shown an induced nestin expression in astrocytes and Müller glial cells peaking at 1 day after KA injection. This was followed by marked BLBP or DCX immunoexpression in astrocytes and Müller glial cells coupled with GFAP expression at 3–14 days post-injection. In parallel with the findings of Raymond et al. (2006), the present data have provided further evidence that rodent astrocytes and Müller glial cells affected by retinal damage would de-differentiate and reacquire an immature molecular profile (expression of nestin, DCX and BLBP). The outcome of this injury-induced glial de-differentiation may be a reconstruction

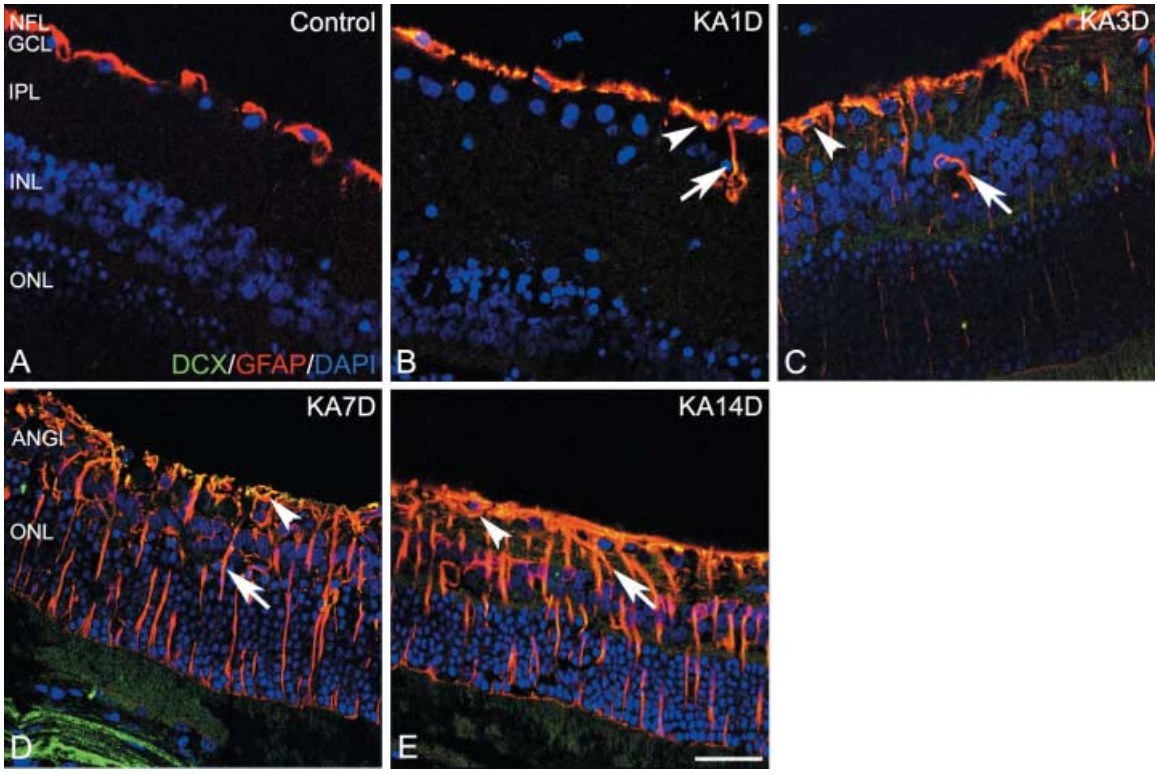

Fig. 10 Confocal images of GFAP (red) and DCX (green) immunolabelling in retinas after saline (A) or KA (B–E) injections. DCX staining is absent in the control retina (A). After KA injection, astrocytes and Müller glial cells positive for GFAP also display DCX immunoreactivity that are mostly localized in the cell processes (B–E, arrows). Immunoreactivities are also detected in some cell bodies in the inner retina (B–E, arrowheads). Abbreviations as in Figs 1 and 2; scale bar = 40 μm.

of retinal stem cell niche of the cell itself (Raymond et al. 2006). The possibility that de-differentiated glia re-creating a microenvironment to support regenerative cascades should be considered.

Conclusion

This study has shown that kainate induces retinal astrocyte and Müller glial cell activation as manifested by an increase in GFAP and nestin expression. The induced nestin expression along with the increased expression of GFAP in astrocytes and Müller glial cells may reflect a metabolic change of the cells in response to the degenerative changes of their neighbouring neurons, the functions of which are closely linked. Injury-induced BrdU incorporation into astrocytes and Müller glial cells indicated their re-entry into the cell cycle. Hence, it is speculated that the induced nestin expression together with GFAP as demonstrated in this study may elicit gliotic responses alongside de-differentiation, which may be related to repair efforts in KA-induced damage. In addition, co-expression of GFAP, BLBP and DCX in astrocytes and Müller glial cells further emphasize that they are endowed with a de-differentiation potential after KA-induced retinal degeneration.

Acknowledgement

This study was supported in part by research grants (NSC 94–2320-B002-002) from the National Science Council, Taiwan.

References

Ahmad I, Tang L, Pham H (2000) Identification of neural progenitors in the adult mammalian eye. *Biochem Biophys Res Commun* **270**, 517–521.

Anthony TE, Klein C, Fishell G, Heintz N (2004) Radial glia serve as neuronal progenitors in all regions of the central nervous system. *Neuron* **41**, 881–890.

Bernreuther C, Salein N, Matschke J, Hagel C (2006) Expression of doublecortin in tumours of the central and peripheral nervous system and in human non-neuronal tissues. *Acta Neuropathol (Berl)* **111**, 247–254.

Bignami A, Dahl D (1979) The radial glia of Müller in the rat retina and their response to injury. An immunofluorescence

study with antibodies to the glial fibrillary acidic (GFA) protein. *Exp Eye Res* **28**, 63–69.

Brown JP, Couillard-Despres S, Cooper-Kuhn CM, Winkler J, Aigner L, Kuhn HG (2003) Transient expression of doublecortin during adult neurogenesis. *J Comp Neurol* **467**, 1–10.

Chen H, Weber AJ (2002) Expression of glial fibrillary acidic protein and glutamine synthetase by Müller cells after optic nerve damage and intravitreal application of brain-derived neurotrophic factor. *Glia* **38**, 115–125.

Damodaran TV, Abou-Donia MB (2000) Alterations in levels of mRNAs coding for glial fibrillary acidic protein (GFAP) and vimentin genes in the central nervous system of hens treated with diisopropylPhosphorofluoridate (DFP). *Neurochem Res* **25**, 809–816.

Daou MC, Smith TW, Litofsky NS, Hsieh CC, Ross AH (2005) Doublecortin is preferentially expressed in invasive human brain tumors. *Acta Neuropathol (Berl)* **110**, 472–480.

Derouiche A, Rauen T (1995) Coincidence of L-glutamate/L-aspartate transporter (GLAST) and glutamine synthetase (GS) immunoreactions in retinal glia: evidence for coupling of GLAST and GS in transmitter clearance. *J Neurosci Res* **41**, 131–143.

Engelhardt M, Wachs FP, Couillard-Despres S, Aigner L (2004) The neurogenic competence of progenitors from the postnatal rat retina in vitro. *Exp Eye Res* **78**, 1025–1036.

Feng L, Hatten MA, Heintz N (1994) Brain lipid-binding protein (BLBP): a novel signaling system in the developing mammalian CNS. *Neuron* **12**, 895–908.

Frederiksen K, McKay RD (1988) Proliferation and differentiation of rat neuroepithelial precursor cells in vivo. *J Neurosci* **8**, 1144–1151.

Frisen J, Johansson CB, Torok C, Risling M, Lendahl U (1995) Rapid, widespread, and longlasting induction of nestin contributes to the generation of glial scar tissue after CNS injury. *J Cell Biol* **131**, 453–464.

Gaughwin PM, Caldwell MA, Anderson JM, et al. (2006) Astrocytes promote neurogenesis from oligodendrocyte precursor cells. *Eur J Neurosci* **23**, 945–956.

Götz M, Barde YA (2005) Radial glial cells: defined and major intermediates between embryonic stem cells and CNS neurons. *Neuron* **46**, 369–372.

Hartfuss E, Galli R, Heins N, Gotz M (2001) Characterization of CNS precursor subtypes and radial glia. *Dev Biol* **229**, 15–30.

Hatten ME (1990) Riding the glial monorail: a common mechanism for glial-guided neuronal migration in different regions of the developing mammalian brain. *Trends Neurosci* **13**, 179–184.

Hatten ME (1999) Central nervous system neuronal migration. *Annu Rev Neurosci* **22**, 511–539.

Hockfield S, McKay R (1985) Identification of major cell classes in the developing mammalian nervous system. *J Neurosci* **5**, 3310–3328.

Honjo M, Tanihara H, Kido N, Inatani M, Okazaki K, Honda Y (2000) Expression of ciliary neurotrophic factor activated by retinal Müller cells in eyes with NMDA- and kainic acid-induced neuronal death. *Invest Ophthalmol Vis Sci* **41**, 552–560.

Kohno H, Sakai T, Kitahara K (2006) Induction of nestin, Ki-67, and cyclin D1 expression in Muller cells after laser injury in adult rat retina. *Graefes Arch Clin Ophthalmol* **244**, 90–95.

Lam TK, Chan WY, Kuang GB, Wei H, Shum AS, Yew DT (1995) Differential expression of glial fibrillary acidic protein (GFAP) in the retinae and visual cortices of rats with experimental renal hypertension. *Neurosci Lett* **198**, 165–168.

Larsen AK, Osborne NN (1996) Involvement of adenosine in retinal ischemia. Studies on the rat. *Invest Ophthalmol Vis Sci* **37**, 2603–2611.

Leavitt BR, Hernit-Grant CS, Macklis JD (1999) Mature astrocytes transform into transitional radial glia within adult mouse neocortex that supports directed migration of transplanted immature neurons. *Exp Neurol* **157**, 43–57.

Lendahl U, Zimmerman LB, McKay R (1990) CNS stem cells express a new class of intermediate filament protein. *Cell* **60**, 585–595.

McDermott KW, Barry DS, McMahon SS (2005) Role of radial glia in cytogenesis, patterning and boundary formation in the developing spinal cord. *J Anat* **207**, 241–250.

Miller SJ, Li H, Rizvi TA, Huang Y, et al. (2003) Brain lipid binding protein in axon–Schwann cell interactions and peripheral nerve tumorigenesis. *Mol Cell Biol* **23**, 2213–2224.

Morest DK, Silver J (2003) Precursors of neurons, neuroglia, and ependymal cells in the CNS: what are they? Where are they from? How do they get where they are going? *Glia* **43**, 6–18.

Newman E, Reichenbach A (1996) The Müller cell: a functional element of the retina. *Trends Neurosci* **19**, 307–312.

Newman EA (2001) Glia of the retina. In *Retina* (ed. Ryan SJ), pp. 89–103. St. Louis: Mosby.

Norton WT, Aquino DA, Hozumi I, Chiu FC, Brosnan CF (1992) Quantitative aspects of reactive gliosis: a review. *Neurochem Res* **17**, 877–885.

Rakic P (1995) Radial versus tangential migration of neuronal clones in the developing cerebral-cortex. *Proc Natl Acad Sci USA* **92**, 11323–11327.

Raymond PA, Barthel LK, Bernardos RL, Perkowski JJ (2006) Molecular characterization of retinal stem cells and their niches in adult zebrafish. *BMC Dev Biol* **6**, 36 [Epub ahead of print].

Ridet JL, Malhotra SK, Privat A, Gage FH (1997) Reactive astrocytes: cellular and molecular cues to biological function. *Trends Neurosci* **20**, 570–577.

Riepe RE, Norenburg MD (1977) Müller cell localization of glutamine synthetase in rat retina. *Nature* **268**, 654–655.

Schmued LC, Albertson CWS Jr (1997) Fluoro-Jade: a novel fluorochrome for the sensitive and reliable histochemical localization of neuronal degeneration. *Brain Res* **751**, 37–46.

Sellner PA (1993) Retinal FABP principally localizes to neurons and not to glial cells. *Mol Cell Biochem* **123**, 121–127.

Sellner P (1994) Developmental regulation of fatty acid binding protein in neural tissue. *Dev Dyn* **200**, 333–339.

Tropepe V, Coles BL, Chiasson BJ, et al. (2000) Retinal stem cells in the adult mammalian eye. *Science* **287**, 2032–2036.

Voigt T (1989) Development of glial-cells in the cerebral wall of ferrets – direct tracing of their transformation from radial glia into astrocytes. *J Comp Neurol* **289**, 74–88.

Walcott JC, Provis JM (2003) Müller cells express the neuronal progenitor cell marker nestin in both differentiated and undifferentiated human foetal retina. *Clin Experiment Ophthalmol* **31**, 246–249.

Xue LP, Lu J, Cao Q, Hu S, Ding P, Ling EA (2006) Müller glial cells express nestin coupled with glial fibrillary acidic protein in experimentally induced glaucoma in the rat retina. *Neuroscience* **139**, 723–732.